ACS MATERIALS LETTERS

Cite This: ACS Materials Lett. 2019, 1, 534–540

www.acsmaterialslett.org

LETTER

Crystallization of a Supramolecular Coassembly of an Atomically Precise Nanoparticle with a Crown Ether

Papri Chakraborty, Abhijit Nag, Korath Shivan Sugi, Tripti Ahuja, Babu Varghese, and Thalappil Pradeep*

Department of Chemistry, DST Unit of Nanoscience and Thematic Unit of Excellence, Indian Institute of Technology Madras, Chennai 600 036, India

Supporting Information

ABSTRACT: We report the crystal structure of a supramolecular coassembly of a red luminescent silver cluster, $[Ag_{29}(BDT)_{12}(TPP)_4]^{3-}$ (referred to as Ag_{29}) (BDT, 1,3-benzene dithiol; TPP, triphenyl phosphine), with dibenzo-18-crown-6 (DB18C6). The structure may be viewed as crystallization-induced self-organization of DB18C6 molecules into cage-like hexamers in the interstitial spaces of the lattice of trigonal Ag_{29} (Ag_{29}T) clusters, which resulted in an anisotropic expansion of the Ag_{29}T lattice along its *z*-axis. This structure corresponds to a new family of "lattice inclusion" compounds in nanoclusters. Supramolecular forces guide the assembly of the clusters and the crown ethers, which pack into complex hierarchical patterns in their crystal lattice. We identified the effect of such a coassembly on the solid-state luminescence of the cluster. The crystals containing the coassembly were ~3.5-fold more luminescent than the parent Ag_{29}T crystals. We also used high-resolution electrospray ionization mass spectrometry to get further insights into the nature of the complexation between Ag_{29} cluster and DB18C6. This study provides a new strategy for designing cluster-assembled functional materials with enhanced properties.

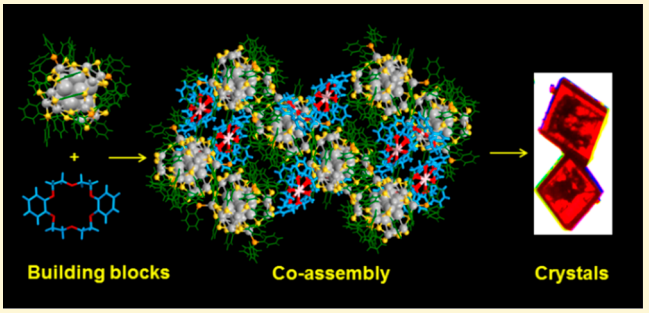

Atomically precise noble metal nanoclusters exhibit a rich diversity in their core and ligand structures.[1−6] Precision in their structure, optical absorption features, and chemical reactivity confirm the molecular nature of such particles.[7,8] Because of their unique physical and chemical properties, they also find applications in sensing, catalysis,[9] and optoelectronics.[10] Noncovalent interactions of the ligands, such as C−H···π, $\pi-\pi$, H-bonding, van der Waals, electrostatic interactions, etc., can induce different forms of assemblies in them.[11] Such interactions also play an important role in organizing the clusters in their crystal lattice.[12−14] Self-organization of the ligands into various patterns was observed in the lattice of $[Au_{246}(p\text{-MBT})_{80}]$,[15] and the packing was similar to that observed in biomolecules. Noncovalent interactions also controlled polymorphism in $[Ag_{29}(BDT)_{12}(TPP)_4]^{3-}$ (BDT, 1,3-benzene dithiol; TPP, triphenyl phosphine) clusters.[16] Extensive H-bonding was observed in the lattice of the cluster, $[Ag_{44}(p\text{-MBA})_{30}]^{4-}$ (*p*-MBA, para mercapto benzoic acid).[12] Self-organization of $[Au_{102}(p\text{-MBA})_{44}]$ clusters into colloidal sheets and capsids were also driven by weak supramolecular forces.[17] Moreover, noncovalent interactions were decisive in determining the assemblies formed by clusters with cyclodextrins (CDs)[18,19] and fullerenes.[20,21] Mathew et al. showed that supramolecular functionalization of $[Au_{25}(SBB)_{18}]^-$ (SBB is 4-(*t*-butyl)benzyl mercaptan) clusters with CDs increased the stability of the cluster core and enhanced the luminescence of the cluster.[18] Nag et al. demonstrated that supramolecular complexation can lead to the emergence of interesting properties like isomerism in nanoclusters.[19] Such reports reveal the growing interest in supramolecular chemistry of atomically precise clusters.[11,22] Though supramolecular assemblies of clusters have been studied using different techniques, such as mass spectrometry, spectroscopy, transmission electron microscopy, theoretical calculations, etc.,[11] the complete structures of the supramolecular adducts of clusters have not yet been solved with atomic precision.

Crown ethers are an interesting class of heterocyclic compounds, which are well-known to form a wide variety of supramolecular host-guest complexes.[23−26] They possess a hydrophilic cavity of ether oxygen atoms which is capable of

Received: August 27, 2019
Accepted: October 8, 2019
Published: October 8, 2019

DOI: 10.1021/acsmaterialslett.9b00352
ACS Materials Lett. 2019, 1, 534–540

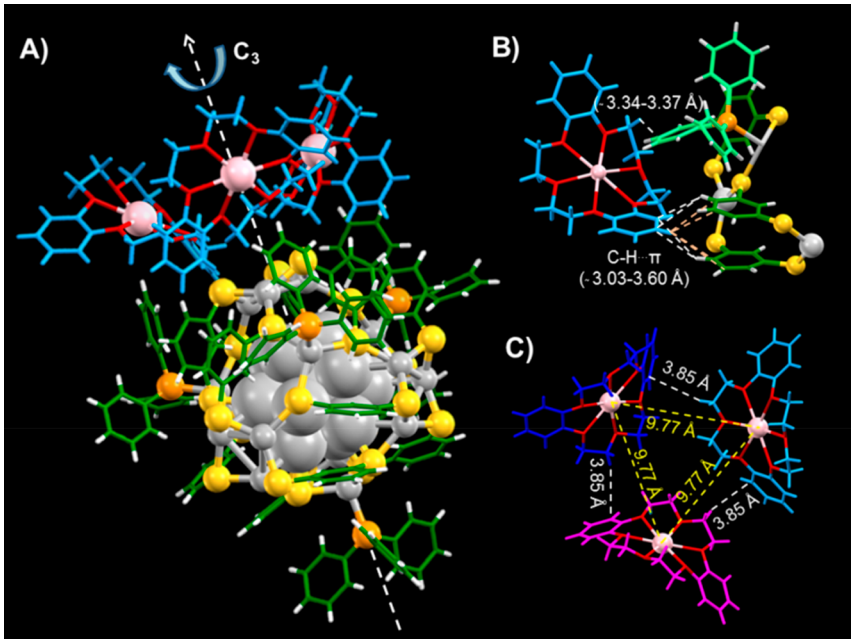

Figure 1. (A) Structure of I, (B) expanded view showing the interaction between one of the DB18C6Na$^+$ molecules and BDT and TPP ligands of the cluster, and (C) expanded view of the three DB18C6Na$^+$ molecules attached on the cluster surface. Color codes: gray, Ag; yellow, S; orange, P; red, O; green, C of BDT and TPP; white, H of BDT and TPP; light blue, C and H of DB18C6; pink, Na. In panel C, C and H of the three DB18C6Na$^+$ molecules are colored differently in light blue, dark blue, and purple, respectively.

capturing alkali and alkaline earth metal ions, and surrounding this cavity there are hydrophobic ethylenic groups. Functionalized crown ethers have also been designed due to the possibilities of new properties that can be generated in them.[27] Due to such properties, crown ethers find numerous applications in phase-transfer catalysis,[26] ion transport mechanism,[28] and as building blocks for supramolecular assemblies.[25] Supramolecular architectures resulting from the interaction of functionalized crown ethers with polyoxometallates have been examined.[29,30] Recently, Guy et al. reported that molybdenum cluster salts, such as A_2MoX_{14} (A = Cs/K and X = Cl/Br), can interact with functionalized 15-crown-5 and assemble into liquid crystalline phases with strong NIR emission.[31] Such studies suggest the potential of using crown ethers as building blocks for designing advanced functional materials.

Herein, we resolved the crystal structure of a supramolecular coassembly of an atomically precise red luminescent cluster, $[Ag_{29}(BDT)_{12}(TPP)_4]^{3-}$ (referred to as Ag_{29})[32] with dibenzo-18-crown-6 (DB18C6). By using single-crystal X-ray diffraction (SCXRD), we show that the crown ethers self-organized into cage-like hexamers in the void spaces of the lattice of Ag_{29} clusters. This resulted in an anisotropic expansion of the lattice of the parent cluster. We also investigated the effect of such a coassembly on the solid-state luminescence of the cluster and investigated the mechanism of assembly formation by using high-resolution electrospray ionization mass spectrometry (ESI MS).

Ag_{29} cluster was chosen as the model cluster system for this study due to its high stability and luminescence properties. The cluster was synthesized following a reported protocol[32] and characterized using optical absorption and ESI MS (Figure S1). Vapor diffusion of methanol into a dimethylformamide solution of Ag_{29} and DB18C6 resulted in the formation of dark red crystals (Figure S2) containing the coassembly of the two entities. Details of synthesis and crystallization are presented in Supporting Information. SCXRD revealed the existence of two molecules, $[Ag_{29}(BDT)_{12}(TPP)_4][(DB18C6Na)_3]$ (**I**) and $[Ag_{29}(BDT)_{12}(TPP)][(DB18C6Na)_3]$ (**II**), with a relative occupancy of 0.765:0.235 in the crystal lattice. The crystal structure of **I** is shown in Figure 1A. Three DB18C6Na$^+$ molecules were assembled over one of the Ag_3S_3 faces of the cluster and oriented symmetrically around the C_3 axis of **I**, which passed through the center of the icosahedron of the cluster and the Ag−P bond opposite to the Ag_3S_3 face. As crown ethers bind to alkali metal ions, Na^+ was trapped in the cavity of DB18C6.[33] Though Na^+ was not added externally during the crystallization process, the source of Na^+ was probably $NaBH_4$ used for cluster synthesis. Intermolecular C−H···π interactions between DB18C6Na$^+$ and the BDT and TPP ligands of the cluster existed in the crystal structure. Moreover, electrostatic interactions between the anionic Ag_{29} cluster and the three cationic units, DB18C6Na$^+$, favored the crystallization. An expanded view showing the interactions between one DB18C6Na$^+$ molecule and the neighboring BDT and TPP ligands of the cluster is presented in Figure 1B. One of the benzene rings of DB18C6Na$^+$ comes in close proximity to a pair of BDT ligands of the cluster, and interacted by intense C−H···π contacts at distances of ∼3.03−3.60 Å, which is comparable to the interaction distances observed in other supramolecular adducts of clusters.[11] The C−H of the $-CH_2$ group of DB18C6Na$^+$ also interacted with the aromatic ring of a TPP ligand at a distance of ∼3.34−3.37 Å. The three DB18C6Na$^+$ molecules, attached on the cluster surface, also interacted between themselves through intermolecular C−H···π contacts at interaction distances of ∼3.85 Å (Figure 1C). The Na^+ at the center of three crown ethers were oriented in a triangular fashion with a distance of 9.77 Å between them, as shown in Figure 1C, and the 3-fold symmetry axis of **I** passed through the center of this triangle. In addition, H_2O was also coordinated to Na^+ with a Na−O distance of ∼2.33 Å (Figure S3). **II** also showed similar geometry but it contained only one

DOI: 10.1021/acsmaterialslett.9b00352
ACS Materials Lett. 2019, 1, 534−540

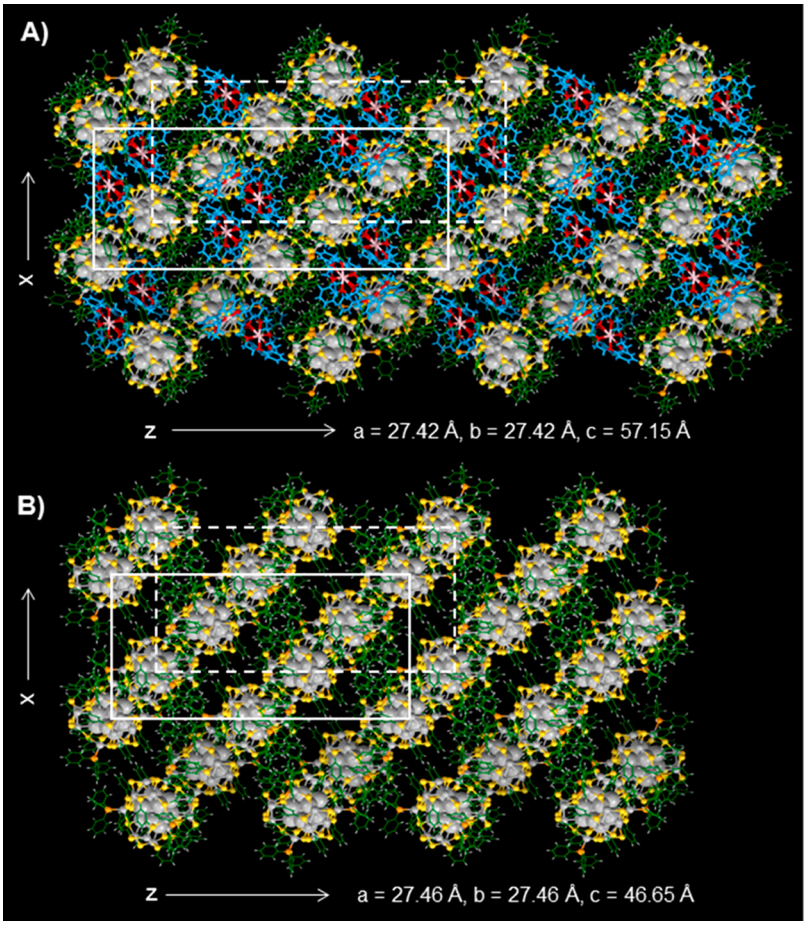

Figure 2. Crystallographic packing of (A) I and (B) $Ag_{29}T$, viewed from *y*-axis.

TPP ligand, which is opposite to the site of attachment of the crown ethers (Figure S4). Due to the labile binding of the TPP ligands of Ag_{29} cluster, some of them were lost during crystallization to form **II**, which constituted a minor component in the crystal lattice. The structure was also carefully explored to find whether any meaningful disorder or inexplicable connectivity existed at any other part of the structure. But none could be found, indicating that no other molecule/fragment existed in the lattice. Further details on solving the crystal structure is presented in the supporting information (Table S1).

A mixture of **I** and **II** crystallized into a single crystal in the trigonal crystal system and $R\bar{3}$ space group. **I** and **II** share the same site in X-ray structure of which 76.5% of the sites in the crystal are occupied by **I** and 23.5% are occupied by **II**. The crystal containing the mixture of **I** and **II** is referred to as Ag_{29}-DB18C6 in the following discussion. The packing of Ag_{29}-DB18C6 was comparable to the packing of the trigonal polymorph of Ag_{29} clusters ($Ag_{29}T$).[16] Along the *z*-axis, the unit cell was elongated to 57.15 Å in case of Ag_{29}-DB18C6, compared to 46.65 Å in case of $Ag_{29}T$, whereas the dimensions along the *x*- and *y*-axis were similar in both cases. This expansion of the lattice along one direction expanded the volume of the unit cell to 37,225 $Å^3$, from the unit cell volume of 30,474 $Å^3$ of $Ag_{29}T$.[16] Anisotropic expansion of the crystal lattice by the inclusion of guest molecules was also observed in the case of inclusion of gases in the lattice of clathrate hydrates.[34] A view of the packing of **I** and $Ag_{29}T$ from the *y*-axis, presented in Figure 2A and B, revealed that the interstitial spaces in the lattice of $Ag_{29}T$ were occupied by DB18C6. The crown ethers were packed in between the clusters by C−H···π contacts, which increased the inter-cluster distances by ∼0.53 nm along *z*-axis, compared to that of $Ag_{29}T$. The nature of packing was similar when viewed from the *x*-axis (Figure S5). A view from the *z*-axis showed that the void spaces along the *z*-axis of $Ag_{29}T$ were occupied by the crown ethers in the case of **I** (Figure S6). The packing of **II** was also similar. The extensive interlocking of ligands in the lattice of Ag_{29}-DB18C6 resulted in a densely packed structure. Moreover, the crown ethers were assembled into discrete hexameric units throughout the crystal lattice, view from the *y*-axis is presented in Figure 3A. The formation of these hexamers of crown ethers was favored by local intermolecular C−H···π contacts and the symmetry of the crystal packing. An expanded view of one such unit, $(DB18C6Na)_6^{6+}$, presented in Figure 3B, reveals that each hexamer formed a hollow cage-like structure, where the pairs of opposite crown ethers on the surface of the cage were related by a centre of inversion. The six Na atoms of the cage were oriented in rectangular bipyramidal geometry (Figure 3C). Six water molecules were trapped inside the cavity of these supramolecular cages (Figure S7). Similar molecular cages were also observed in the case of hexameric assemblies of resorcarenes,[35] calixarenes,[36] insulin,[37] etc., and such cages usually act as hosts for trapping guest molecules,[38] and also as molecular capsules for catalyzing certain reactions.[39] Thus, crystal structure of Ag_{29}-DB18C6 may be described as a "lattice inclusion compound" or "lattice clathrate",[40] where guest molecules (crown ether hexamers) get crystallized in the

DOI: 10.1021/acsmaterialslett.9b00352
ACS Materials Lett. 2019, 1, 534−540

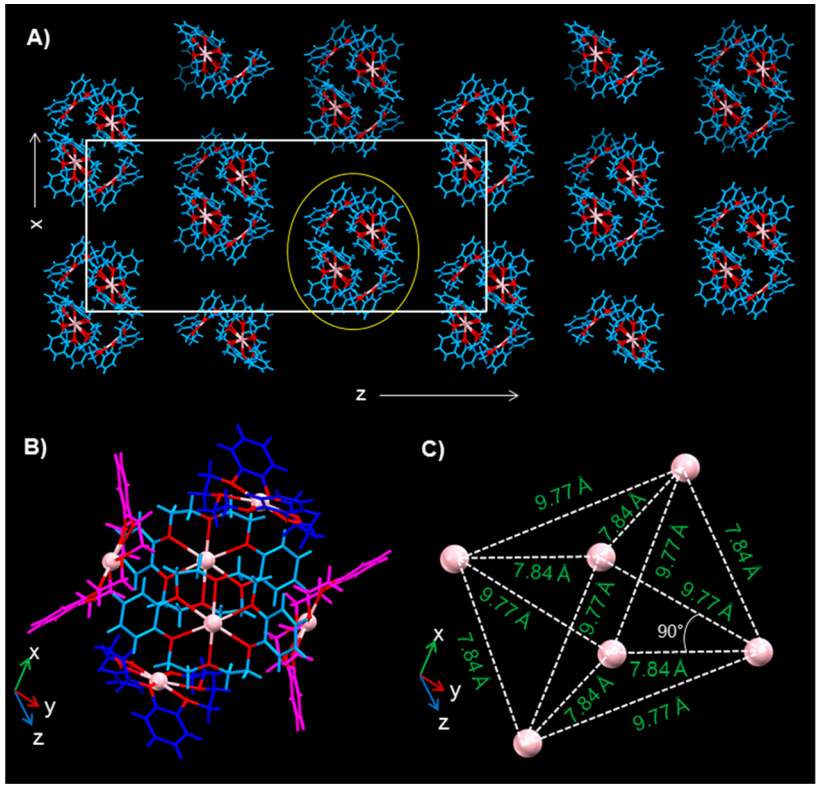

Figure 3. (A) Packing of DB18C6Na$^+$ molecules into hexameric units throughout the crystal lattice, view from the *y*-axis. (B) Expanded view of one of the hexameric units (circled in yellow in A) showing the formation of cage-like structures. Opposite crown ethers, shown in similar colors, are related by a center of inversion. (C) The orientation of the Na$^+$ of the crown ether hexamer in a rectangular bipyramidal geometry.

interstitial spaces of the host lattice ($Ag_{29}T$) and depending on the size of the guest molecules, expansion of the crystal lattice occurs. Such a phenomenon was not observed earlier in the case of nanoclusters.

In the structure of **I**/**II**, two types of host-guest interactions may be visualized: first, at the molecular level where crown ethers trap Na^+ and secondly, complexation of these crown ethers with the cluster, where the cluster can be considered as a colloidal-level molecule. Moreover, from the packing of Ag_{29}-DB18C6, it is evident that Ag_{29} clusters and DB18C6 molecules show hierarchical assembly in their crystal lattice. While the lattice of the cluster acts as a host for trapping the crown ether cages, these cages further act as a host for trapping water as the guest molecules. Further, the cages themselves are formed by self-organization of six DB18C6Na$^+$ units and each DB18C6Na$^+$ unit is formed by the capture of Na^+ in the cavity of DB18C6. In the crystal lattice, there are cluster−cluster, crown ether−crown ether, and cluster−crown ether interactions. Supramolecular forces guide the assembly behavior at each level. The packing patterns represent an emerging phenomenon in nanoscience where simple building blocks evolve into complex architectures with new features that are not manifested in individual entities.

We compared the emission from both Ag_{29}-DB18C6 and $Ag_{29}T$ to understand the effect of the noncovalent interactions on their solid-state luminescence. Though the density of the particles in Ag_{29}-DB18C6 (∼1.85 gm cm^{-3}), was slightly less compared to the density in the lattice of $Ag_{29}T$ (∼2.041 gm cm^{-3}), there was ∼3.5 fold enhancement in the luminescence of the former (excitation at 532 nm). Details of the luminescence measurements and calculation of enhancement factors are discussed under the experimental section in the Supporting Information. Dense packing of the ligands in the case of Ag_{29}-DB18C6 resulted in greater rigidity and restriction of the intramolecular rotations of the TPP ligands which caused an enhancement of the radiative transitions,[16,41,42] compared to the lattice of $Ag_{29}T$. Ion pairing effects of the negatively charged clusters with the positively charged DB18C6Na$^+$ in their crystal may have also contributed to the enhancement of the luminescence.[43] The slight red shift and broadening in the emission spectrum of Ag_{29}-DB18C6 may be attributed to changes in electronic coupling and electron-phonon interactions[32] in the two crystals. Despite the structural complexity of the inclusion compound (Ag_{29}-DB18C6), the uniformity in the properties of the single crystal makes the luminescence comparison possible. Similar phenomenon was also observed in the case of the polymorphic crystals of the cluster where the cubic polymorph ($Ag_{29}C$) exhibited a more rigid packing and higher luminescence compared to $Ag_{29}T$.[16] The Ag_{29}-DB18C6 crystals were more luminescent compared to $Ag_{29}C$ (density ∼ 2.11 g cm^{-3}) too (Figure S8). However, when Ag_{29}-DB18C6 crystals were dissolved in DMF, there was no change in the emission compared to the solution-phase emission of the parent Ag_{29} clusters (Figure S9A), which further supported that the enhancement was due to the strong intermolecular interactions in the crystalline state and in solution-phase such intermolecular interactions were lost due to random arrangement of the molecules. The optical absorption features were also unchanged compared to that of the parent cluster (Figure S9B), which suggested weak interaction between the molecules in solution.

DOI: 10.1021/acsmaterialslett.9b00352
ACS Materials Lett. 2019, 1, 534−540

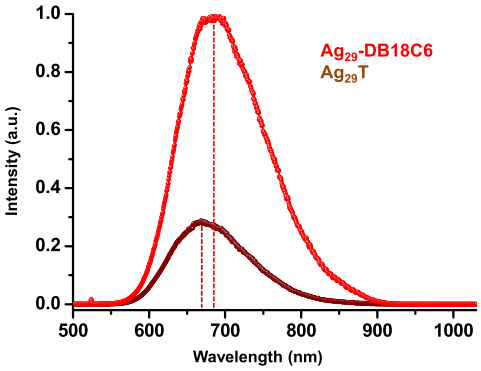

Figure 4. Emission from Ag_{29}-DB18C6 and Ag_{29}T crystals, excited at 532 nm.

To understand the nature of solution-phase complexation, we dissolved the Ag_{29}-DB18C6 crystals in DMF and analysed these by ESI MS. In the negative ion mode, the adducts, $[Ag_{29}(BDT)_{12}(TPP)_n(DB18C6)_m]^{3-}$ (n = 0−4, m = 0−3) were detected (Figure 5). The peaks are labelled with (n, m)

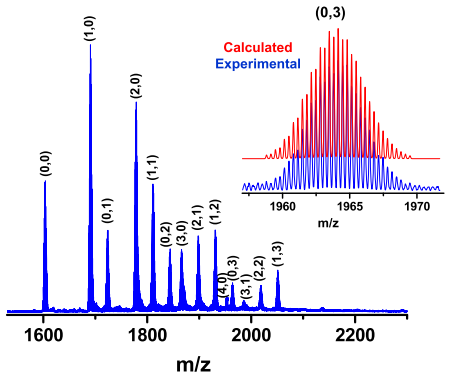

Figure 5. ESI MS from the crystals of coassemblies of Ag_{29} cluster and DB18C6, dissolved in DMF, in negative mode showing the detection of the adducts, $[Ag_{29}(BDT)_{12}(TPP)_n(DB18C6)_m]^{3-}$ (n = 0−4, m = 0−3). The comparison of the theoretical and experimental isotopic distribution patterns of $[Ag_{29}(BDT)_{12}(DB18C6)_3]^{3-}$ is shown in the inset. The labels (x,y) means x = number of TPP (n) and y = number of DB18C6 molecules (m) attached to the cluster.

indices. As the TPP ligands were labile and DB18C6 molecules were noncovalently bound, they were detached from the cluster during ionization. This complicated the exact quantification of the adducts and the abundances of the species could not be compared with their occupancy in the crystal structure. However, a maximum of three DB18C6 molecules was found to be attached to the cluster with varying number of TPP ligands. Moreover, in the positive ion mode, the species, $DB18C6Na^+$ was detected (Figure S10). This suggested the existence of two types of equilibria in solution: (i) attachment of neutral DB18C6 to the cluster and (ii) capture of Na^+ by DB18C6. Both these processes contributed to the crystallization of Ag_{29}-DB18C6.

In summary, we crystallized a supramolecular coassembly of Ag_{29} and DB18C6 molecules. The structure showed an anisotropic expansion of the parent Ag_{29}T lattice due to the incorporation of DB18C6 hexamers in the interstitial spaces of its lattice. The crystals of the coassembly of Ag_{29} with DB18C6 exhibited greater luminescence compared to the crystals of the parent Ag_{29}T. This supramolecule may find application as a luminescent probe for selective cation sensing. The hexameric cages of crown ethers in the crystal lattice may also be utilized for trapping gases or other suitable guest molecules. Similar interactions may also be explored for a range of different clusters and crown ethers. The crystallization of such supramolecular assemblies of clusters unfolds a new direction in nanoparticle engineering and such functional materials may show enhanced optical and mechanical properties. By choosing the appropriate crown ether, cluster assembled liquid crystalline phases may be created, which may find applications in optoelectronic devices. As crown ethers are sensitive to all alkali metal ions, others, such as Li^+, may be incorporated in the nanoparticle assemblies and these modified materials may find applications in electrochemical devices. Noble metal cluster assemblies assisted by crown ethers are expected to enhance the area.

■ ASSOCIATED CONTENT

Supporting Information

The Supporting Information is available free of charge on the ACS Publications website at DOI: 10.1021/acsmaterialslett.9b00352.

Materials and methods, crystal structure data, optical absorption and emission, and ESI MS (PDF)

Crystallographic information file for Ag_{29}-DB18C6 (CIF)

■ AUTHOR INFORMATION

Corresponding Author

*E-mail: pradeep@iitm.ac.in.

ORCID

Thalappil Pradeep: 0000-0003-3174-534X

Notes

The authors declare no competing financial interest.

CCDC 1888965 contains the crystallographic data for this paper. These data are provided free of charge by The Cambridge Crystallographic Data Centre.

■ ACKNOWLEDGMENTS

P.C. thanks the Council of Scientific and Industrial Research (CSIR) for a research fellowship. A.N. and T.A. thank IITM for their fellowship. K.S.S. thanks the University Grants Commission (UGC) for her fellowship. We thank the Department of Science and Technology, Government of India, for continuously supporting our research programme. We thank the Sophisticated Analytical Instruments Facility, IITM, for SCXRD data collection. Authors thank Dr. Sudhadevi Antharjanam for useful discussions on the SCXRD data.

■ REFERENCES

(1) Chakraborty, I.; Pradeep, T. Atomically Precise Clusters of Noble Metals: Emerging Link between Atoms and Nanoparticles. *Chem. Rev.* **2017**, *117*, 8208−8271.

(2) Jin, R.; Zeng, C.; Zhou, M.; Chen, Y. Atomically Precise Colloidal Metal Nanoclusters and Nanoparticles: Fundamentals and Opportunities. *Chem. Rev.* **2016**, *116*, 10346−10413.

(3) Yao, Q.; Chen, T.; Yuan, X.; Xie, J. Toward Total Synthesis of Thiolate-Protected Metal Nanoclusters. *Acc. Chem. Res.* **2018**, *51*, 1338−1348.

DOI: 10.1021/acsmaterialslett.9b00352
ACS Materials Lett. 2019, 1, 534−540

(4) Maity, P.; Xie, S.; Yamauchi, M.; Tsukuda, T. Stabilized Gold Clusters: From Isolation toward Controlled Synthesis. *Nanoscale* **2012**, *4*, 4027−4037.
(5) Ghosh, A.; Mohammed, O. F.; Bakr, O. M. Atomic-Level Doping of Metal Clusters. *Acc. Chem. Res.* **2018**, *51*, 3094−3103.
(6) Krishnadas, K. R.; Natarajan, G.; Baksi, A.; Ghosh, A.; Khatun, E.; Pradeep, T. Metal−Ligand Interface in the Chemical Reactions of Ligand-Protected Noble Metal Clusters. *Langmuir* **2019**, *35*, 11243−11254.
(7) Krishnadas, K. R.; Baksi, A.; Ghosh, A.; Natarajan, G.; Som, A.; Pradeep, T. Interparticle reactions: An Emerging Direction in Nanomaterials Chemistry. *Acc. Chem. Res.* **2017**, *50*, 1988−1996.
(8) Natarajan, G.; Mathew, A.; Negishi, Y.; Whetten, R. L.; Pradeep, T. A Unified Framework for Understanding the Structure and Modifications of Atomically Precise Monolayer Protected Gold Clusters. *J. Phys. Chem. C* **2015**, *119*, 27768−27785.
(9) Higaki, T.; Li, Y.; Zhao, S.; Li, Q.; Li, S.; Du, X.-S.; Yang, S.; Chai, J.; Jin, R. Atomically Tailored Gold Nanoclusters for Catalytic Application. *Angew. Chem.* **2019**, *131*, 8377−8388.
(10) Mathew, A.; Pradeep, T. Noble Metal Clusters: Applications in Energy, Environment, and Biology. *Part. Part. Syst. Char.* **2014**, *31*, 1017−1053.
(11) Chakraborty, P.; Nag, A.; Chakraborty, A.; Pradeep, T. Approaching Materials with Atomic Precision using Supramolecular Cluster Assemblies. *Acc. Chem. Res.* **2019**, *52*, 2−11.
(12) Yoon, B.; Luedtke, W. D.; Barnett, R. N.; Gao, J.; Desireddy, A.; Conn, B. E.; Bigioni, T.; Landman, U. Hydrogen-Bonded Structure and Mechanical Chiral Response of a Silver Nanoparticle Superlattice. *Nat. Mater.* **2014**, *13*, 807.
(13) Yao, Q.; Yu, Y.; Yuan, X.; Yu, Y.; Zhao, D.; Xie, J.; Lee, J. Y. Counterion-Assisted Shaping of Nanocluster Supracrystals. *Angew. Chem., Int. Ed.* **2015**, *54*, 184−189.
(14) Li, Q.; Russell, J. C.; Luo, T.-Y.; Roy, X.; Rosi, N. L.; Zhu, Y.; Jin, R. Modulating the Hierarchical Fibrous Assembly of Au Nanoparticles with Atomic Precision. *Nat. Commun.* **2018**, *9*, 3871.
(15) Zeng, C.; Chen, Y.; Kirschbaum, K.; Lambright, K. J.; Jin, R. Emergence of Hierarchical Structural Complexities in Nanoparticles and their Assembly. *Science* **2016**, *354*, 1580−1584.
(16) Nag, A.; Chakraborty, P.; Bodiuzzaman, M.; Ahuja, T.; Antharjanam, S.; Pradeep, T. Polymorphism of $Ag_{29}(BDT)_{12}(TPP)_4^{3-}$ Cluster: Interactions of Secondary Ligands and their Effect on Solid State Luminescence. *Nanoscale* **2018**, *10*, 9851−9855.
(17) Nonappa; Lahtinen, T.; Haataja, J. S.; Tero, T.-R.; Häkkinen, H.; Ikkala, O. Template-Free Supracolloidal Self-Assembly of Atomically Precise Gold Nanoclusters: From 2D Colloidal Crystals to Spherical Capsids. *Angew. Chem., Int. Ed.* **2016**, *55*, 16035−16038.
(18) Mathew, A.; Natarajan, G.; Lehtovaara, L.; Häkkinen, H.; Kumar, R. M.; Subramanian, V.; Jaleel, A.; Pradeep, T. Supramolecular Functionalization and Concomitant Enhancement in Properties of Au_{25} Clusters. *ACS Nano* **2014**, *8*, 139−152.
(19) Nag, A.; Chakraborty, P.; Paramasivam, G.; Bodiuzzaman, M.; Natarajan, G.; Pradeep, T. Isomerism in Supramolecular Adducts of Atomically Precise Nanoparticles. *J. Am. Chem. Soc.* **2018**, *140*, 13590−13593.
(20) Chakraborty, P.; Nag, A.; Paramasivam, G.; Natarajan, G.; Pradeep, T. Fullerene-Functionalized Monolayer-Protected Silver Clusters: $[Ag_{29}(BDT)_{12}(C_{60})_n]^{3-}$ (n = 1−9). *ACS Nano* **2018**, *12*, 2415−2425.
(21) Ahmed, G. H.; Parida, M. R.; Tosato, A.; AbdulHalim, L. G.; Usman, A.; Alsulami, Q. A.; Murali, B.; Alarousu, E.; Bakr, O. M.; Mohammed, O. F. The Impact of Electrostatic Interactions on Ultrafast Charge Transfer at Ag_{29} Nanoclusters−Fullerene and CdTe Quantum Dots−Fullerene Interfaces. *J. Mater. Chem. C* **2016**, *4*, 2894−2900.
(22) Nonappa; Ikkala, O. Hydrogen Bonding Directed Colloidal Self-Assembly of Nanoparticles into 2D Crystals, Capsids, and Supracolloidal Assemblies. *Adv. Funct. Mater.* **2018**, *28*, 1704328.
(23) Gokel, G. W.; Leevy, W. M.; Weber, M. E. Crown Ethers: Sensors for Ions and Molecular Scaffolds for Materials and Biological Models. *Chem. Rev.* **2004**, *104*, 2723−2750.
(24) Elbasyouny, A.; Bruegge, H. J.; Von Deuten, K.; Dickel, M.; Knochel, A.; Koch, K. U.; Kopf, J.; Melzer, D.; Rudolph, G. Host-Guest Complexes of 18-Crown-6 with Neutral Molecules Possessing the Structure Element XH_2 (X = Oxygen, Nitrogen, or Carbon). *J. Am. Chem. Soc.* **1983**, *105*, 6568−6577.
(25) Liu, Z.; Nalluri, S. K. M.; Stoddart, J. F. Surveying Macrocyclic Chemistry: From Flexible Crown Ethers to Rigid Cyclophanes. *Chem. Soc. Rev.* **2017**, *46*, 2459−2478.
(26) Hiraoka, M. *Crown Ethers and Analogous Compounds*; Elsevier Science & Technology Books, 1992.
(27) Shinkai, S. *Functionalization of Crown Ethers and Calixarenes: New Applications as Ligands, Carriers, and Host Molecules*; Springer: Berlin, 1990; pp 161−195.
(28) He, G.-X.; Kurita, M.; Ishii, I.; Wada, F.; Matsuda, T. New Applications of Crown Ethers. 11. Structural Effect of the Counter Anion on Crown-Ether Mediated Cation Extraction and Transport. A Direct Examination of the Crown Ether-Cation Complex in the Organic Phase of Extraction and Transport. *J. Membr. Sci.* **1992**, *69*, 61−73.
(29) You, W.; Wang, E.; Xu, Y.; Li, Y.; Xu, L.; Hu, C. An Alkali Metal−Crown Ether Complex Supported by a Keggin Anion through the Three Terminal Oxygen Atoms in a Single M_3O_{13} Triplet: Synthesis and Characterization of $[\{Na(Dibenzo\text{-}18\text{-}Crown\text{-}6)(MeCN)\}_3\{PMo_{12}O_{40}\}]$. *Inorg. Chem.* **2001**, *40*, 5468−5471.
(30) Akutagawa, T.; Endo, D.; Noro, S.-I.; Cronin, L.; Nakamura, T. Directing Organic−Inorganic Hybrid Molecular-Assemblies of Polyoxometalate Crown-Ether Complexes with Supramolecular Cations. *Coord. Chem. Rev.* **2007**, *251*, 2547−2561.
(31) Guy, K.; Ehni, P.; Paofai, S.; Forschner, R.; Roiland, C.; Amela-Cortes, M.; Cordier, S.; Laschat, S.; Molard, Y. Lord of the Crowns: A New Precious in the Kingdom of Clustomesogens. *Angew. Chem., Int. Ed.* **2018**, *57*, 11692−11696.
(32) AbdulHalim, L. G.; Bootharaju, M. S.; Tang, Q.; Del Gobbo, S.; AbdulHalim, R. G.; Eddaoudi, M.; Jiang, D.-e.; Bakr, O. M. $Ag_{29}(BDT)_{12}(TPP)_4$: A Tetravalent Nanocluster. *J. Am. Chem. Soc.* **2015**, *137*, 11970−11975.
(33) Li, Y.; Wang, E.; Wang, S.; Lu, Y.; Hu, C.; Hu, N.; Jia, H. Synthesis, Characterization and Crystal Structures of Dibenzo-18-Crown-6 Sodium Isopolytungstates. *J. Mol. Struct.* **2002**, *607*, 133−141.
(34) Murayama, K.; Takeya, S.; Alavi, S.; Ohmura, R. Anisotropic Lattice Expansion of Structure of Clathrate Hydrates Induced by Help Guest: Experiments and Molecular Dynamics Simulations. *J. Phys. Chem. C* **2014**, *118*, 21323−21330.
(35) Wierzbicki, M.; Głowacka, A. A.; Szymański, M. P.; Szumna, A. A Chiral Member of the Family of Organic Hexameric Cages. *Chem. Commun.* **2017**, *53*, 5200−5203.
(36) Pasquale, S.; Sattin, S.; Escudero-Adán, E. C.; Martínez-Belmonte, M.; de Mendoza, J. Giant Regular Polyhedra from Calixarene Carboxylates and Uranyl. *Nat. Commun.* **2012**, *3*, 785.
(37) Smith, G. D.; Swenson, D. C.; Dodson, E. J.; Dodson, G. G.; Reynolds, C. D. Structural Stability in the 4-Zinc Human Insulin Hexamer. *Proc. Natl. Acad. Sci. U. S. A.* **1984**, *81*, 7093−7097.
(38) Liu, L.; Zhang, Y.; Wang, X.-L.; Luo, G.-G.; Xiao, Z.-J.; Cheng, L.; Dai, J.-C. Supramolecular Network of Triaminotriptycene and its Water Cluster Guest: Synthesis, Structure, and Characterization of $[(tatp)_4{\cdot}17H_2O]_n$. *Cryst. Growth Des.* **2018**, *18*, 1629−1635.
(39) Bolliger, J. L. Self-Assembled Coordination Cages and Organic Capsules as Catalytic Supramolecular Reaction Vessels. *Effects of Nanoconfinement on Catalysis*; Poli, R., Ed.; Springer International Publishing: Cham, 2017; pp 17−48.
(40) Bishop, R. Designing New Lattice Inclusion Hosts. *Chem. Soc. Rev.* **1996**, *25*, 311−319.
(41) Khatun, E.; Ghosh, A.; Chakraborty, P.; Singh, P.; Bodiuzzaman, M.; Ganesan, P.; Nataranjan, G.; Ghosh, J.; Pal, S. K.; Pradeep, T. A Thirty-fold Photoluminescence Enhancement

DOI: 10.1021/acsmaterialslett.9b00352
ACS Materials Lett. 2019, 1, 534−540

Induced by Secondary Ligands in Monolayer Protected Silver Clusters. *Nanoscale* **2018**, *10*, 20033−20042.
(42) Chandra, S.; Nonappa; Beaune, G.; Som, A.; Zhou, S.; Lahtinen, J.; Jiang, H.; Timonen, J. V. I.; Ikkala, O.; Ras, R. H. A. Highly Luminescent Gold Nanocluster Frameworks. *Adv. Opt. Mater.* **2019**, 1900620.
(43) Bootharaju, M. S.; Kozlov, S. M.; Cao, Z.; Shkurenko, A.; El-Zohry, A. M.; Mohammed, O. F.; Eddaoudi, M.; Bakr, O. M.; Cavallo, L.; Basset, J.-M. Tailoring the Crystal Structure of Nanoclusters Unveiled High Photoluminescence *via* Ion Pairing. *Chem. Mater.* **2018**, *30*, 2719−2725.

DOI: 10.1021/acsmaterialslett.9b00352
ACS Materials Lett. 2019, 1, 534−540